Water-use by fast-growing *Eucalyptus grandis* x *E. nitens* clonal hybrid and *Pinus elliottii* near the Two Streams Research Catchment, South Africa

Nkosinathi D. Kaptein[1], Colin S. Everson[2,4], Alistair D. Clulow[1,2], Michele L. Toucher[2,3], Ilaria Germishuizen[5]

[1]Discipline of Agrometeorology, University of KwaZulu-Natal, Pietermaritzburg, 3209, South Africa
[2]Centre for Water Resources Research, University of KwaZulu-Natal, Pietermaritzburg, 3209, South Africa
[3]Grasslands-Forests-Wetlands Node, South African Environmental Observation Network, Pietermaritzburg, 3201, South Africa
[4]Department Plant and Soil Sciences, University of Pretoria, Pretoria, South Africa

[5]Institute for Commercial Forestry Research, Scottsville, 3201, South Africa

Correspondence to: Nkosinathi D. Kaptein (kapteinnd@gmail.com)

Abstract. Pine plantations are the dominant specie currently planted within the South African commercial forestry industry. Improvements in bioeconomy markets for dissolving wood pulp products have seen an expansion in fast-growing *Eucalyptus* plantations due to their higher productivity rates and better pulping properties than pine. This has raised concerns regarding the expansion of *Eucalyptus* plantations and how they will affect water resources as they have been reported to have higher water use (quantified using transpiration rates, T) than pine. We measured T (mm), diameter at breast height (quantified as quadratic mean diameter, D_q, m) and leaf area index (LAI) of an eight-year-old *Eucalyptus grandis* x *Eucalyptus nitens* clonal hybrid (GN) and a twenty-year-old *Pinus elliottii*. Transpiration was measured for two consecutive hydrological years (2019' 20 and 2020' 21) using a heat ratio sap-flow method calibrated against the lysimeter. In the 2019' 20 year, annual T for *P. elliottii* exceeded GN by 28%, while 2020' 21 hydrological year showed no significant differences. This was associated with 17 and 21% greater LAI for *P. elliottii* than GN in 2019' 20 and 2020' 21 measurement years, respectively. D_q increments were statistically similar ($p > 0.05$) in 2019' 20, whereas the 2020' 21 year produced significant differences ($p < 0.05$). Transpiration for *P. elliottii* responded linearly to solar radiation and the LAI ($R^2 > 0.70$), while GN T responded well only to solar radiation ($R^2 > 0.70$). The profile water content recharge was influenced by rainfall events. After rainfall and soil profile water recharge, there was a rapid depletion of soil water by the GN trees, while the soil profile was depleted more gradually at the *P. elliottii* site after rainfall events. As a result, trees in the GN site appeared to be water stressed, suggesting that there was no alternative water source for trees to access. The study concluded that 1) *P. elliottii* can use more water than GN (depending on soil water stress conditions of the site) 2) commercial forest plantations may deplete soil water stored within the soil profile, resulting in streamflow reduction over a long term. However, long-term total soil water balance studies are recommended in the same region to understand the long-term impact of commercial plantations on water resources.

1 Introduction

The expansion of new areas of commercial afforestation in South Africa have generally slowed in recent years in favour of the composition of existing plantations changing. This decrease has been attributed to political, environmental and climate change influences (Nambiar, 2019). Pine plantations are still the dominant species in South Africa occupying approximately 49.6% of total commercial forest plantation areas (Forestry South Africa, 2018). These plantations are mainly grown for sawlog (74.7%) and coarse-fibre pulpwood (24.9%). Over the years, there has been an improvement in the bioeconomy market for dissolving wood pulp products such as short fine-fibre pulp. Fast-growing *Eucalyptus* species are now being considered an alternative to pine due to their superior fibre and pulping properties (Dougherty and Wright, 2012), short rotation (8-12 years) and high productivity rates (Albaugh et al., 2013). *Eucalyptus* plantation productivity can be as high as 35 m^3 ha^{-1} $year^{-1}$ on highly productive sites compared to 25-27 m^3 ha^{-1} $year^{-1}$ of pine (Fox et al., 2007). As a result, over the past 10 years, the areas planted to pine in South Africa have decreased by 2% while *Eucalyptus* increased by 10% (Forestry South Africa, 2018). There are now plans to replace as many as 300 000 ha of pine with *Eucalyptus* over the next 20 years (Forestry South Africa, 2018).

The potential for an increase in planting *Eucalyptus* species in South Africa may present several environmental considerations including a potential impact to biodiversity (Callaham et al., 2013) and high rates of transpiration (T) and total evaporation (Stanturf et al., 2013). There is a wide body of knowledge indicating that *Eucalyptus* species T is greater than pine (Scott and Lesch, 1997; Albaugh et al., 2013) and can reduce off-site water yield (Calder, 2002). Given the imminent increase in *Eucalyptus* plantations in the near future, it is vital to understand water use by pine and *Eucalyptus*. A *Eucalyptus grandis* versus *Pinus patula* comparison by Scott and Lesch (1997) on very deep soils, found that *E. grandis* used up to 100 mm more water per year than *P. patula* using streamflow measurements. In contrast, White et al. (2021), reported no annual differences between T of *E. globulus* and *P. radiata* in central Chile.

Pinus elliottii and *E. grandis* x *Eucalyptus nitens* clonal hybrid (*GN*) are the second and fourth most planted species in South Africa, respectively. There is no existing literature that quantifies T by these two species in South Africa and mixed reports in the international literature. The objective of this study was therefore to measure T (as an indicator of tree water use) of *GN* and *P. elliottii* plantations and the impact posed by each species on plantation water yield. Transpiration for both species were measured in the same stage of development (same rotational age), therefore, the *P. elliottii* plantation (age 20 years old) was 12 years older than *GN* (8 years old).

2 Methods

2.1 Description of study area

The study area was located on the Mistley Canema estate (29°12'19.78"S, 30°39'3.78"E) in the KwaZulu-Natal midlands of South Africa, which is about 70 km north-east of Pietermaritzburg (Fig. 1). The area is generally hilly with rolling landscapes and a high percentage of arable land (Everson et al., 2014). It is dominated by forb-rich, tall, sour *Themeda triandra* grasslands

65 of which only a few patches remain due to invasion of native *Aristida junciformis*. Soils in this area are highly leached with apedal and plinthic soil forms, mostly derived from the Ecca group with dolerite dykes and sills. The area experiences mist which could significantly contribute to overall precipitation through streamflow or canopy interception (Mucina and Rutherford, 2006). Weather events such as moderate frost, droughts, hail, and berg winds are frequent in the area.

2.2 Site description

70 The study sites were located adjacent to the Two Stream Research Catchment used in previous (Clulow et al., 2011; Everson et al., 2014) forestry research (Fig. 1). Study site 1 was situated on the north-western side of the catchment (1.6 km away) and planted to *GN* in August of 2013. Study site 2 (3.5 km away from the catchment) was established in August 2001 and planted to *Pinus elliottii*. Basic characteristics for both study sites are presented in Table 1. Research by Clulow et al. (2011) and Everson et al. (2014) at Two Streams Research Catchment classified the soil profile to be as deep as 13 m (Table 2) and below

75 that consists of a weathered bedrock (saprolite) and fractured basement rock. The soil form was classified as Hutton (Soil Classification Working Group 1991). Study sites were 4 km away from each other with the automatic weather station located approximately equidistant between the two sites. Both *GN* and *P. elliottii* were planted at a spacing of 2 x 3 m (1667 trees ha^{-1}). The *GN* trees were established using cuttings, while for *P. elliottii*, seedlings were used. Both study sites were subjected to standard afforestation practices such as pruning and thinning, weeding pre-canopy closure and slash removal every 5th row to

80 minimise fire risk.

2.3 Environmental monitoring

An automatic weather station (AWS) was installed on a flat uniform grassland area in the middle of the two study sites to provide supporting meteorological measurements. Measurements of air temperature (T_{air}, °C) (HMP 60, Vaisala Inc., Helsinki, Finland), the relative humidity (RH, %) (HMP60, Vaisala Inc., Helsinki, Finland), the wind speed (m s^{-1}) and direction

85 (degrees) (Model 03003, R.M. Young, Traverse City, Michigan, USA), the solar radiation (I_s, MJ m^{-2} day^{-1}) (Kipp and Zonen CMP3) and rainfall (mm day^{-1}) (TE525, Texas Electronics Inc., Dallas, Tx, USA) were conducted every 10 s and output hourly. The sensors were installed according to recommendations of the World Meteorological Organisation (WMO, 2010) with the rain gauge orifice at 1.2 m and the remaining sensors at 2 m above the ground surface. The sensor outputs were recorded on a CR1000 datalogger. The datalogger (Campbell Scientific Inc., Logan, Utah, USA) recorded 5-min outputs and was

90 programmed to calculate the Vapour Pressure Deficit (VPD, kPa) using T_{air} and RH measurements according to Savage et al. (1997).

2.4 Transpiration flux measurements

Four representative trees were selected within each study site based on diameter stratification. This was achieved by measuring 48 tree diameters at breast height (DBH, 1.3 m) using a diameter tape and stratifying the measured trees according to four size

95 classes; small, medium, medium large and large.

The heat ratio method of a heat pulse velocity system (HPV) (Burgess et al., 2001) was used to estimate sap-flow at various depths across the sap-wood of each selected tree for the 2019' 20 (October 2019 to October 2020) and 2020' 21 hydrological years (October 2020 to October 2021). The HPV system consisted of a line heater probe (4 cm long and of 0.18 cm outside diameter brass tubing) with enclosed constantan filament that provides a heat source for 0.5 s when powered and a pair of type T copper-constantan thermocouples to measure the heat ratio. For *Pinus elliottii* trees, slightly longer heater probes (6 cm) were used due to the xylem being situated deeper in coniferous trees when compared to angiosperm trees. Prior to probe installation, thickness of the bark was measured, and suitable sensor insertion depth was identified using an increment borer and Methyl Orange staining. The thermocouples and heater probes were inserted in holes, which were made using a drill and a drill guide to ensure that holes were drilled with the correct spacing and parallel alignment. A heater probe was installed in the central hole and thermocouples installed in each of the holes up (upstream) and down (downstream) from the heater probe relative to the sap-flow direction. Probes were installed at various depths (Table 3) within a tree. Hourly measurements were executed and recorded using a CR1000 datalogger (Campbell Scientific Inc.) powered by a single 55-amp hour lead acid deep cycle battery. Thermocouples were connected to an AM 16/32 multiplexer (Campbell Scientific Inc.), which was in turn connected to a CR1000 datalogger to allow for 32 measurements at various sap-wood depths across the four instrumented trees. Data were remotely downloaded using a GSM modem (Maestro Wireless Solutions Ltd. Hong Kong, China)

Hourly measurements started by measuring each thermocouple ten times for accurate initial temperatures. Following a heat pulse, the downstream and upstream temperatures were measured 40 times between 60 and 100s. Thereafter, heat pulse velocity (V_h, cm hr^{-1}) was calculated using (Burgess et al., 2001),

$$V_h = \frac{k}{x} \ln\left(\frac{V_1}{V_2}\right) 3600 \qquad (1)$$

Where k is a thermal diffusivity of fresh wood (a nominal value of 2.5 x 10^{-3} cm^2 s^1), x is the distance of each temperature probe from heater probe (cm), and V_1 and V_2 are temperature increases in upstream and downstream probe (°C) at equidistant points.

A slight probe misalignment may occur during the drilling process even when a drill guide is used. This was assessed by checking for inconsistencies in the zero flux values in periods where sap-flow was expected to be zero, such as over pre-dawn, during rainfall events, or in high *RH* and low soil water content (*SWC*) conditions. The sap-flow values during these times were adjusted to zero and an offset calculated from an average of these values and applied to the whole dataset. For probes used in this study, the offset was < 5% of the midday sap-flow rates.

Wounding or non-sap conducting area around the thermocouples was accounted for using wound correction coefficients described by Burgess et al. (2001). Thereafter, sap velocities were calculated accounting for moisture fraction and wood density as described by Burgess et al. (2001). Finally, sap velocities were converted to *T* rates (mm day^{-1}) by summing products of sap velocity and cross-sectional area for individual stems. The *T* rates were then weighted as per individual tree contribution to provide a measure of whole stand *T*.

2.5 Soil water content measurements

130 At both sites hourly SWC was measured in the upper 0.60 m of the soil profile (0.20 m, 0.40 m and 0.60 m depth) using CS616 soil water measuring sensors (Campbell Scientific Inc.). The CS616 SWC sensor consists of two 30 cm long stainless-steel rods that uses the time domain reflectometer method to measure the SWC. The sensor circuitry generates an electromagnetic pulse, of which an elapsed pulse travel time and reflection are measured and then used to calculate the SWC. Research conducted at Two Streams Catchment (Clulow et al., 2011; Everson et al., 2014) reported that the majority of large and fine

135 roots were located in the top 0.06 m to 0.4 m of the soil profile, hence SWC measurements were conducted in the top 0.6 m of the soil profile in our study. The SWC measurements ran concurrently with the sap-flow measurements and were recorded on the CR1000 datalogger. The profile water content at 0.6 m soil depth ($PWC_{0.6}$) was estimated from the SWC measurements using:

140 $$PWC_{0.6} = (SWC_{0.2} \times 0.2) + (SWC_{0.4} \times 0.2) + (SWC_{0.6} \times 0.2) \hspace{2cm} (2)$$

where, $SWC_{0.2}$, $SWC_{0.4}$, $SWC_{0.6}$ was the soil water content measured at 0.2 m, 0.4 m and 0.6 m, respectively.

2.6 Heat ratio technique calibration

The HPV method is an internationally recognised and reliable technique for measuring individual tree T in uniform stands

145 (Hatton and Wu, 1995; Meiresonne et al., 1995; Crosbie et al., 2007). There are however difficulties, bringing uncertainty to the accuracy of the absolute sap-flow results, such as the anisotropic sap-wood properties (Vandegehuchte et al., 2012), radial patterns of the sap-flow (Cermák and Nadezhdina, 1998), tree symmetry (Vertessy et al., 1997) and changes in spatial patterns of T (Traver et al., 2010). Some studies have indicated that the technique underestimates sap-flow in *Eucalyptus* by as much as 45% (Maier et al., 2017; Fuchs et al., 2017), whereas pine may be overestimated by as much as 49% (Dye et al., 1996b).

150 This necessitated a calibration experiment to validate the field measurements.

The calibration experiment was conducted in an open area at the Institute for Commercial Forestry Research nursery, located at the University of KwaZulu-Natal, Pietermaritzburg for a period of 30 days as illustrated in Figure 2. Two-year-old GN and four-year-old *Pinus elliottii* trees grown in 25-L plastic containers (diameter=36 cm, height = 42 cm) filled with vermiculite

155 were sourced from Mondi Mountain Home Estate nursery (Hilton, South Africa). The containers had holes at the base (to allow for drainage) and were placed on a rubber mat with slots to prevent root contact with soil and to allow water to drain away from the container. Twenty-four hours before starting the experiment, both trees were well watered, and each container was insulated using plastic at the tree base to prevent soil evaporation and induce water loss solely through T. Tree diameters at the start of an experiment were 0.044 and 0.036 m for GN an *P. elliottii*, respectively. Each tree was instrumented with HPV

160 sensors to measure hourly sap-flow (as discussed in section 2.4) and summed from sunrise to sunset to make up daily tree T

(L day^{-1}). Concurrently, each soil container was weighed in the morning and afternoon, using a lysimeter (resolution=0.001g, placed on a flat concrete surface to ensure it remains level during the experiment) to determine daily changes in container weight (kg, where 1 kg was assumed to be equivalent to 1 L) as a measure of T. This process was repeated for five days to get a calibration over a range of plant available water values, whereafter trees were again well-watered (achieved by removing insulation plastic) and allowed to drain completely before restarting measurements. Sapwood area and wounding was accounted for according to Burgess et al. (2001) to derive daily T. A simple regression was conducted between daily T and daily change in tree mass.

2.7 Growth measurements

Measurements of DBH were conducted monthly using manual dendrometer bands (D1, UMS, Muchin, Germany) permanently attached to a tree, with an accuracy of 0.1 mm. Dendrometer bands were installed at beginning of October 2019 on 48 trees including the four HPV instrumented trees and data were manually collected for 21 months. The quadratic mean diameter (D_q) was calculated for 48 trees using (Curtis and Marshall, 2000):

$$D_q = \sqrt{\frac{\overline{(\Sigma(d^2))}}{n}} \tag{3}$$

where; d is the DBH (m) of an individual tree and n is the total number of trees. Tree heights for the 48 trees were measured simultaneously using a hypsometer (Vertex Laser VL402, Haglof, Sweden). Monthly measurements of leaf area index (LAI) were conducted using a LAI-2200 Plant Canopy Analyzer (Licor Inc., Lincoln, New York, USA) on a 0.6 ha transect that was identified through the middle of each study site from October 2019 to October 2021.

2.8 Statistical analysis

Analysis of variance (ANOVA) was used to analyse species differences in stand characteristics (T, D_q, tree heights and LAI) using the R version 3.6.1 statistical package. Variables were transformed as appropriate to meet the assumptions of normality. Where the overall F-statistic was significant ($p < 0.05$), treatment means were compared using Fischer's Least Significant Difference at the 5% level of significance (LSD$_{5\%}$). Statistical parameters that were used included the regression co-efficient (R^2), root mean square error (RMSE), standard error of a regression slope (SE slope), standard error of the intercept (SE intercept) and a ratio of variance of y-intercept to x-intercept (F).

3 Results

3.1 Automatic weather station

The minimum and maximum daily T_{air} were typical of the 30-year average of Mistley Canema. Maximum recorded T_{air} was 36.5 and 37.5°C for 2019' 20 and 2020' 21 hydrological years, respectively. There were several days where T_{air} were below freezing between May and July for both measurement years (Fig. 3a). Rainfall between 01 October 2019 and 30 September

2020 amounted to 857 mm and 825 mm for 01 October 2020 to September 2021. Majority of this rainfall (70%) fell during summer months (November to March) for both years (Fig. 3d). By comparison, ET_0 totals calculated using hourly AWS data and the FAO56 method (Allen et al., 1998) amounted to 1100 mm and 1056 mm for 2019' 20 and 2020' 21 hydrological years, respectively. Daily maximum VPD was 3.08 kPa for 2019' 20 increasing to 3.53 kPa for 2020' 21 year during hot summer months (Fig. 3c). Monthly average wind speed ranged from 2.2 to 7.7 m s^{-1} over the two hydrological years with maximum wind speeds up to 37 m s^{-1} in August/ September. The RH reached 100% during the night, decreasing to as low as 20% during the day on hot summer months. Average I_s for 2019' 20 and 2020' 21 hydrological years was 15.5 and 16 MJ m^{-2} day^{-1}, respectively, while both years experienced a maximum I_s of 30 MJ m^{-2} day^{-1} in summer (Fig. 3b).

3.2 Soil profile water content

The $PWC_{0.6}$ was very responsive to rainfall events (Figure 4) on both study sites. The peak $PWC_{0.6}$ for the GN site during the wet season was 227 mm and 198 mm in 2019' 20 and 2020' 21 hydrological years, respectively. By comparison, the maximum measured $PWC_{0.6}$ in the *P. elliottii* site was 128 mm day^{-1} in 2019' 20 and 125 mm day^{-1} in 2020' 21. The $PWC_{0.6}$ at both study sites did not significantly respond to rainfall events below 5 mm hr^{-1}, except during consecutive rainfall events. After a significant rainfall event, the $PWC_{0.6}$ for the GN site was depleted rapidly, within hours (Figure 4), which contrasts with the *P. elliottii* site, where $PWC_{0.6}$ was depleted more gradually, lasting for a few days post the rainfall event. The swift depletion of plant available water at the GN site, resulted in the site experiencing extended periods of very low profile water content. During the dry season, the $PWC_{0.6}$ was maintained at approximately 50 and 60 mm day^{-1} for *P. elliottii* and GN, respectively, except when significant rainfall events occurred.

Commercial forest plantations are known to have a very deep rooting system and are able to access soil water in deeper soil water reserves (Christina et al. 2016). A study adjacent to our study site (Everson et al. 2014) reported that *Acacia mearnsii* tree roots were as deep as 8 m into the soil profile. Similar results were reported by Dye (1996) in the Mpumalanga province of South Africa, where *Eucalyptus grandis* trees abstracted water down to 8 m below the soil surface. The deep soil profile with the presence of weathered bedrock (saprolite) in our study site suggests that trees were capable of rooting as deep as 20 m into the soil profile and were probably restricted by the bedrock (grey fine-grained shale). However, Hasenmueller et al. (2017) indicated that shale may consist of fractures where tree roots may grow through. There is, therefore, a high possibility that tree roots in this study accessed soil water stored deep in the soil profile from previous wet years.

3.3 Heat ratio calibration

The HPV system slightly overestimated T (in the case of the GN) and underestimated T (in the case of the *P. elliotii*) when compared to a lysimeter system. A simple regression between the two systems produced a good linear relationship (GN:

R^2=0.73, *P. elliottii*: R^2=0.76) for both tree species (Fig. 5a and 5b), with a RMSE of 0.57 and 0.36 L day^{-1} for the *GN* and *P. elliottii*, respectively. This relationship was used to correct the *T* results for both tree species:

$$GN = 1.17x - 0.011 \hspace{4cm} (4)$$
$$P.\ elliottii = 0.81x + 0.11 \hspace{4cm} (5)$$

3.4 Transpiration rates

The *T* followed typical seasonal and diurnal pattern for both sites in both 2019' 20 and 2020' 21 hydrological years (Fig. 6). *Pinus elliottii* had significantly ($p < 0.01$) higher mean daily *T* compared to *GN* (Fig. 6) except for the winter of 2021 (May to August) where *GN* was statistically (p=0.012) greater. Mean daily *T* values in summer of 2019' 20 for *Pinus elliottii* and *GN* were 2.5 and 1.9 mm day^{-1}, respectively. By comparison, summer mean *T* values of 2020' 21 were 2.6 mm day^{-1} for *P. elliottii* and 2.1 mm day^{-1} for *GN* ($p < 0.05$). After a significant rainfall event (~5 mm hr^{-1}), *T* for *GN* momentarily exceeded *P. elliottii* for a few days, thereafter, falling below *P. elliottii*. The maximum *T* for *GN* was 5.2 mm day^{-1} and 3.8 mm day^{-1} for 2019' 20 and 2020' 21 measurement year, respectively, versus 5.6 mm day^{-1} for *P. elliottii* in both seasons. During 2019' 20, *GN* reached peak *T* rates early in summer (late December 2019) compared to *P. elliottii*, where peak *T* rates were measured in late January to early February of 2020 (Fig. 6). However, maximum *T* rates were reached mid-January for the 2020' 21 measurement year by both crops, which coincided with high *I$_s$*, *T$_{air}$* and VPD. During winter months (June to July) of both the 2019' 20 and 2020' 21 hydrological years no *T* could be detected by probes on *GN* trees on several days, despite clear weather conditions. This corresponded with low *PWC$_{0.6}$* (approximately 60 mm day^{-1} per 0.6 m soil depth). By comparison, *T* could be measured in *P. elliottii* trees where the *PWC$_{0.6}$* was low (~ 50 mm day^{-1} per 0.6 m soil depth), however at very low *T* rates (~0.33 mm day^{-1}). Following rainfall, the *P. elliottii* response to *PAW* lagged behind the *GN* trees. While *GN T* increased almost immediately, *P. elliottii T* only responded a few days later (Fig. 7).

The differences in seasonal patterns of *T* are better illustrated using daily accumulated *T* as presented in Fig. 8. Over the 2019' 20 measurement year, the total accumulated daily *T* for *P. elliottii* was 30% greater than *GN*, while the total accumulated rainfall exceeded *P. elliottii* and *GN T* by 21 mm year^{-1} and 258 mm year^{-1}, respectively (Fig. 8). In comparison, the total accumulated *T* rates in 2020' 21 were statistically similar ($p > 0.05$) throughout the year with accumulated rainfall 18 and 20% greater than *T* for *P. elliottii* and *GN*, respectively. The accumulated *ET$_o$* exceeded rainfall by 22% in both seasons. Total annual *T* rates for *GN* were slightly higher in 2020' 21 than 2019' 20 measurement years by 6%, while *P. elliottii T* rates reduced by 19% during the same period (Fig. 8).

3.5 Response to climatic variables

Tree *T* for each species was compared by multiple regression analysis to micrometeorological parameters including *I$_s$*, VPD, rainfall, *RH*, wind speed and *T$_{air}$* to determine individual and combined drivers of *T*. The most responsive variable was *I$_s$* for

both tree species, where an increase in I_s resulted to an increase in T ($R^2 > 0.75$), except in winter of 2019' 20 for GN and 2020' 21 for *P. elliottii* (Table 4). VPD significantly influenced GN T only in the summer months for both measurement years, where a 2nd order polynomial relationship was produced ($R^2 > 0.62$). Transpiration increased with an increase in VPD, up to a threshold of approximately 2.8 mm day^{-1}, thereafter remaining constant (data not shown). In addition, there was hysteresis in GN, where at similar VPD, T was greater in the morning than in the afternoon. By comparison, *P. elliottii* showed no significant response to VPD on both measurement years (Table 4). Tree T was also highly correlated with RH in *P. elliottii*, where T increased with decrease in RH, reaching a peak of 2.5 mm day^{-1} (RH=21%) and 5.6 mm day^{-1} (RH=23%) in 2019' 20 (winter) and 2020' 21 (summer), respectively. Rainfall, wind speed and T_{air} did not significantly influence T of both species.

3.6 Tree growth

At the beginning of the study, *P. elliottii* trees were larger in diameter than GN. There was a seasonal pattern in D_q increment by both species (Fig. 9), with no significant ($p > 0.05$) differences in 2019' 20, while 2020' 21 produced significantly ($p < 0.05$) greater growth increment in *P. elliottii* than GN. Interestingly, a negative growth increment was measured during the winter of 2019' 20 for GN, which was probably caused by low $PWC_{0.6}$.

3.7 Leaf area index

The mean summer LAI for *P. elliottii* was 17% greater than GN (*P. elliottii*=2.5 vs GN=2.05, $p < 0.05$) in 2019' 20 increasing to 21% (*P. elliottii*=3.1 vs GN=2.4, $p < 0.05$) in 2020' 21. Winter LAI decreased to 1.31 and 1.76 for *P. elliottii* and GN, respectively. Total monthly T was linearly related to monthly LAI of both *P. elliottii* and GN (Fig. 10), with statistical differences in the regression ($p < 0.05$). However, there was a greater RMSE, SE intercept and SE slope in *P. elliotti* than in GN.

4 Discussion

4.1 Daily T

The *P. elliottii* mean daily T exceeded GN by about 24% over the 2019' 20 and by 19% in 2020' 21 measurement years, mainly influenced by I_s and RH. Differences in T between GN and *P. elliottii* could be attributed to the following reasons: 1) trees at the GN site were water stressed and evidence of water stress was observed through shrinking of tree stem diameters during winter, zero rates of T on some days during winter months and a significant decrease in LAI over winter. This suggests that trees were unable to access soil water stored from previous wet years held deep in the soil profile or the GN trees had already accessed and depleted the stored soil water before the study period. *Eucalyptus* T has been shown to increase sharply in the early stages of growth, reaching a peak in the middle of the rotation, thereafter, declining as the stand matures (Delzon and Loustau 2005). With our GN trees 8-years-old (full rotation is 12 years), it is most likely that soil water was depleted in the early years of the rotation 2) sap-wood for *P. elliottii* was nearly twice the sap-wood area of GN due to the different tree

structures. The *GN* mean *T* range of 0.9–5.2 mm day^{-1} and 0.5–3.8 mm day^{-1} for 2019' 20 and 2020' 21, respectively, measured in this study agreed with *Eucalyptus* studies in relatively low rainfall areas with trees of the same age. For example, a study by Forrester et al. (2010) on seven-year-old *E. globulus* in Australia measured a *T* range of 0.4–1.9 mm day^{-1} (MAP=708 mm). David et al. (1997) measured daily *T* of 0.5–3.64 mm day^{-1} at a *E. globulus* site in Portugal with a MAP of 600 mm. A South African study by Dye et al. (1996a) on nine-year-old *E. grandis* in Mpumalanga, South Africa measured *T* of 2.0–7.5 mm day^{-1} with the potential to exceed 8.0 mm day^{-1} under high VPD (Dye et al., 2013), however, this study was conducted in a high rainfall area (MAP=1459), with almost double the MAP of the current study. For *P. elliottii*, peak *T* of 5.6 mm day^{-1} in this study agreed with other studies, such as Hatton and Vertessy (1990) who measured a maximum *T* of 5 mm day^{-1} in *P. radiata* in new South Wales, Australia.

During summer *GN T* peaked earlier than the *P. elliottii* (more distinct in 2019' 20) and then decreased swiftly, so that it was less than the *P. elliottii T* in the late summer to early autumn. In addition, the *GN T* increased sharply after the rainfall events and thereafter decreased as *PWC$_{0.6}$* was rapidly depleted, while *P. elliottii* responded more gradually. This suggests that *GN* trees have a different growth and water use strategy to *P. elliottii,* that involves using available water rapidly. A similar observation was reported by White et al. (2021) from *E. globulus* in central Chile. This implies that *GN* trees compete for water and use it more rapidly when it becomes available, and this strategy can expose them to extreme water stress if soil water deficit conditions persist as reported by Mitchell et al. (2013). *P. elliottii* had a greater *T* at stem sizes similar to the *GN* (ie. *D$_q$* for smallest *P. elliottii* tree versus *D$_q$* for largest *GN* tree). This may be attributed to a markedly smaller heartwood in *P. elliottii* than *GN*. However, it should be noted that pine trees consist of several latewood rings in which no sap movement occurs (Dye et al., 2001). Diurnal changes in *T* typically lagged behind VPD, creating a pattern of hysteresis, where at similar VPD, *T* was greater in the morning than in the afternoon for *GN*. Studies by O'Grady et al. (1999) and Maier et al. (2017) attributed this to low soil hydraulic conductivity or the use of stored stem water for *T* in the first portion of the day. Further analysis in our study indicated that *GN T* was significantly influenced by VPD only in summer, suggesting that water stress may have affected water uptake to a greater extent in winter.

4.2 Annual T

On an annual basis, *P. elliottii* trees transpired 28% more water (836 mm) than *GN* (599 mm) in 2019' 20, while the 2020' 21 saw no significant differences between the two species (*P. elliottii*=678 mm vs. *GN*=639 mm). The low rates of *T* in winter months (May to August) of 2021 on the *P. elliotti* site (Fig. 6), were caused by low *SWC*, which resulted in similar annual *T* rates in 2020' 21 by both species. *Pinus* studies (Moran et al., 2017; Samuelson et al., 2019) reported that the first reaction by pine species to a decrease in *SWC* is a significant reduction in stomatal aperture, causing a decrease or cessation of *T*. By comparison, *GN* indicated a different response, where *T* continued (even when *SWC* was marginally limiting) to a point where it was below detection by our HPV system and this trait makes eucalypts vulnerable during extended or severe drought periods. Similar findings were reported by White et al., (1999) and Eksteen et al., (2013) in *E. nitens*, where trees utilised *SWC* till

315 permanent wilting point, which seems to be well beyond the -1500 kPa typically cited in literature for many plants (Santra et al., 2018).

There are contrasting results in some annual comparative studies of T between *Eucalyptus* and *Pinus* species. In an eight-year-old *E. benthamii* vs *P. taeda* comparative water use study in the United States (Maier et al., 2017), annual T of 1077 and 733 mm year^{-1} for *E. benthamii* and *P. taeda*, respectively, were measured. In a South African study (tree water use estimated using

320 water balance), *Eucalyptus grandis* used 100 mm more water per year than *Pinus patula* (Scott and Lesch, 1997). Notwithstanding these findings, another study in southeastern Australia, Benyon and Doody (2015) found no significant differences between annual water use (only T was measured) between *E. globulus* and *P. radiata*, with or without access to groundwater. A most recent study by White et al. (2022) using meta-analysis of published evapotranspiration estimates found no significant differences in water use between *Eucalyptus* and *Pinus* genera. Like other studies (Whitehead and Beadle, 2004;

325 Samuelson et al., 2008), a strong correlation between T and LAI was observed in this study, with *P. elliottii* having a greater T rate than *GN* at a similar LAI. This good correlation may present a modelling opportunity to estimate T using site measurements of LAI or remote sensing estimates of LAI.

4.3 Implications of tree water use on water yield

Our results indicated that *P. elliottii* T was significantly greater than *GN* in 2019' 20, while 2020' 21 T patterns were statistically

330 similar. These results were influenced by *SWC* and physiological response by each specie to soil water shortage. It is most likely that *GN* trees would have used more water than *P. elliottii* if *SWC* was not limiting T or if trees had been able to access groundwater reserves, for example through capillary rise. This conjecture is supported by studies conducted by Calder (1992), Dye et al. (1996a) and O'Grady et al. (1999), where *Eucalyptus* T was higher during the dry season than during the wet season, largely due to exploitation of groundwater reserves.

335 These implications are significant in local planning by the commercial forestry industry, since current markets favour replacement of longer rotation pine with shorter rotation *Eucalyptus* plantations. However, the dry soil profile at the *GN* site compared with the *P. elliottii* could have significant long-term impacts on the water-balance of such forestry catchments. Without comprehensive knowledge of long-term total water balance measurements, the implications over a number of rotations cannot be quantified. Studies have reported a negative effect of *Eucalyptus* on catchment water yield (Almeida et al., 2007),

340 whereas others have reported no significant impact (Lane et al., 2004; White et al., 2021, 2022). A conclusion based on results from our study site, is that commercial forest plantations may deplete soil water stored within the soil profile during dry period, resulting in potential streamflow reduction over a long term. Due to climate variability in plantation forest areas, long-term studies under non-stressed and stressed conditions are needed in this region to quantify the total water balance (total evaporation, surface runoff, soil water storage and how water partitioning responds to climate change and afforestation over

345 time).

5 Conclusions

This paper presents a water use study by *GN* and *P. elliottii* near the Two Streams Research Catchment in the KwaZulu-Natal midlands of South Africa, quantified using the heat ratio method (HRM). Though the HRM is an internationally recognised technique for measuring *T* in commercial forests, tree specific calibration was conducted in this study to validate our water use measurements. Our calibration results indicated that HRM provided reliable and continuous measurements of water use, but require routine maintenance. Annual water use results indicated that *P. elliottii* used 28% more water than *GN* in the first measurement year, while there were no significant differences in *T* in the second year of measurement. These findings contrasted with some previous pine and eucalypts comparative studies conducted in South Africa and internationally, which reported that *Eucalyptus* species are heavy water users compared to pine. There was a good relationship between *T* and LAI and *T* and I_s, indicating that *T* may be influenced by a combination of different growth and weather variables. This relationship will form a good background for modelling studies, where a 'easy-to-measure' growth and weather parameters can be used to estimate a difficult to derive water use measurement.

It was concluded in this study that, in contrast to common misperception, 1) *P. elliottii* can use more water than *GN* (depending on soil water stress), 2) in countries such as South Africa, where streamflow reduction by commercial forestry is modelled, soil water stress in hydrological models must be able to constrain tree water use and that models should accommodate deep rooted trees accessing groundwater reserves through capillary rise in deep soil profiles. Further research is suggested to quantify the total water balance (total evaporation, surface runoff, soil water storage and how water partitioning responds to climate change and afforestation over time).

6 Data availability

Due to the high-frequency data used for this paper, all data with linked figures and tables have been uploaded to the central database at the Centre for Water Resources Research (CWRR) at the University of KwaZulu-Natal in Pietermaritzburg. The author, Nkosinathi David Kaptein, can be contacted for these data at kapteinnd@gmail.com.

7 Author contribution

MLT and ADC were responsible for funding acquisition, resources and project administration. MLT, ADC and CSE conceptualised the study and conceived the methodology. NDK was a student who collected the data, analysed, interpreted, and wrote the original draft of the paper. ADC, MLT, CSE and IG provided student supervision, discussed the results, and contributed to the final version of the paper.

8 Competing interests

The contact author has declared that none of the authors has any competing interests.

9 Acknowledgements

This research was funded by the Department of Water and Sanitation through Water Research Commission. Mondi Group and Mistley Canema Estate are acknowledged for their support in providing access to research sites. David Borain provided invaluable assistance and support. Assistance from Mxolisi Gumede, Xolani Colvelle, Jimmy Nhlangulela was much appreciated.

10 Financial support

This research has been supported by the South African Department of Water and Sanitation through a Water Research Commission project K5/2791.

11 References

Albaugh, J. M., Dye, P. J., King, J. S. 2013: Eucalyptus and water use in South Africa. Int. J. For. Res., 11, 852540, http://doi:10.1155/2013/852540, 2013.

Allen, R. G., Pereira, L. S., Raes, D., and Smith, M.: Crop evapo-transpiration: Guidelines for computing crop water requirements, FAO Irrigation and Drainage Paper 56, Food and Agriculture Organization of the United Nations, Rome, Italy, 1998.

Almeida, A. C., Soares, J. V., Landsberg, J. J., Rezende, G. D.: Growth and water balance of Eucalyptus grandis hybrid plantations in Brazil during a rotation for pulp production, For. Ecol. Manage., 251, 10-21, https://doi.org/10.1016/j.foreco.2007.06.009, 2007.

Benyon, R. G, Doody, T. M.: Comparison of interception, forest floor evaporation and transpiration in *Pinus radiata* and *Eucalyptus globulus* plantations, Hydrol. Process*.,* 29, 1173-1187, https://doi.org/10.1002/hyp.10237, 2014.

Bulcock, H. H., Gush, M. B., Jewitt, G. P. W.: A comparison of productive and non-productive green water-use efficiency of *Podocarpus henkelii* and *Pinus patula* in KwaZulu-Natal Midlands. Southern Forests, 76, 75–84, https://doi.org/10.2989/20702620.2014.915451, 2014.

Burgess, S. S. O., Adams, M. A., Turner, N. C., Beverly, C. R., Ong, C. K., Khan, A. A. H., and Bleby, T. M.: An improved heat pulse method to measure low and reverse rates of sap flow in woody plants, Tree Physiol., 21, 589–598, http://dx.doi.org/10.1093/treephys/21.9.589, 2001.

Curtis, R. O, Marshall, D, D: Why Quadratic Mean Diameter? Pac. Res. Stat., Olympia, Technical Note, 13799., 2000.

Calder, I. R: *Eucalyptus*, water and the environment, In: *Eucalyptus*, edited by: Coppen, J. J. W., Taylor and Francis, Wales, London, 16-23, 2002.

Callaham, M. A., Stanturf, J. A., Hammond, W., Rockwood, D. L., Wenk, E. S., O'Brien, J. J.: Survey to evaluate escape of eucalyptus spp. seedlings from plantations in south eastern USA, Int. J. Forest. Res., 13, http://dx.doi.org/10.1155/2013/946374, 2013.

Canadell, J., Jackson, R. B., Ehleringer, J. B., Mooney, H. A, Sala, O. E., Schulze, E. D.: Maximum rooting depth of vegetation types at the global scale, Oecologia, 108, 583–595, https://doi.org/10.1007/bf00329030, 1996.

Cannell, M. G. R.: Environmental impacts of forest monocultures: water use, wildlife conservation, and carbon storage. New Forest, 17, 239–262, http://10.1007/978-94-017-2689-4_17, 1999.

420

Cermák, J. and Nadezhdina, N.: Sapwood as the scaling parameter- defining according to xylem water content or radial pattern of sap flow?, Ann. For. Sci., 55, 509–521, https://doi.org/10.1051/forest:19980501, 1998.

Christina, M., Nouvellon, Y., Laclau, J. P., Stape, J. L., Bouillet, J. P., Lambais, G. R., Le Maire, G.: Importance of deep-water
425 uptake in tropical eucalypt forest, Funct. Ecol., 31, 509-519, https://doi.org/10.1111/1365-2435.12727, 2016.

Clulow, A. D., Everson, C. S., Gush, M. B.: The long-term impact of *Acacia mearnsii* trees on evaporation, streamflow and groundwater resources, Water Research Commission Report TT 505/11, ISBN 9781431200203, South Africa, 104 pp., 2011.

430 Crosbie, R., Wilson, B., Hughes, J., and McCulloch, C.: The upscaling of transpiration from individual trees to areal transpiration in tree belts, Plant Soil, 297, 223–232, https://doi.org/10.1007/s11104-007-9337-y, 2007.

David, T. S., Ferreira, M. I., David, J. S., Pereira, J. S.: Transpiration from mature *Eucalyptus globulus* plantation in Portugal during a spring -summer period of progressively high-water deficit, Oecologia, 110, 153-159,
435 https://doi.org/10.1007/PL00008812, 1997.

Dougherty, D., Wright, J.: Silviculture and economic evaluation of eucalypt plantations in the Southern US, BioResources, 7, 1994–2001, http://dx.doi.org/10.15376/biores.7.2.1994-2001, 2012.

440 Dye, P. J.: Response of *Eucalyptus grandis* trees to soil water deficits, Tree Physiol., 16, 233–238, http://doi:10.1093/treephys/16.1-2.233, 1996a.

Dye, P. J., Soko, S., Poulter, A. G.: Evaluation of the heat pulse velocity method for measuring sap flow in *Pinus Patula*, J. Exp. Bot., 47, 975–981, https://doi.org/10.1093/jxb/47.7.975, 1996b.
445

Dye, P. J, Poulter, A. G., Soko, S., Maphanga, D.: The determination of the relationship between transpiration rate and declining available water for *Eucalyptus grandis*, Water Research Commission Report No. 441/1/97, ISBN 1868453057, Pretoria, South Africa, 103 pp., 1997.

450 Dye, P. J., Vilakazi, P., Gush, M., Ndlela, R., Royappen, M.: 2001. Investigation of the feasibility of using trunk growth increments to estimate water use of *Eucalyptus grandis* and *Pinus Patula* plantation. Water Research Commission Report No. 809/1/01, ISBN 1868458164, South Africa, 229 pp., 2001.

Dye, P. J., Jacobs, S., Drew, D.: Verification of 3-PG growth and water-use predictions in twelve *Eucalyptus* plantation stands
455 in Zululand, South Africa, For. Ecol. Manage., 193, 197–218, http://dx.doi.org/10.1016/j.foreco.2004.01.030, 2004.

Dye, P. J.: A review of changing perspectives on *Eucalyptus* water-use in South Africa, For. Ecol. Manage., 301, 51-57, http://dx.doi.org/10.1016/j.foreco.2012.08.027, 2013.

460 Eksteen, A. B., Grzeskowiak, V., Jones, N. B., Pammenter, N. W.: Stomatal characteristics of *Eucalyptus grandis* clonal hybrids in response to water stress, South. For., 75, 105-111, https://doi.org/10.2989/20702620.2013.804310, 2013.

Everson, C. S., Clulow, A. D., Becker, M., Watson, A., Ngubo, C., Bulcock, H., Mengistu, M., Lorentz, S., Demlie, M.: The long-term impact of *Acacia mearnsii* trees on evaporation, streamflow, low flows and ground water resources. Phase II:
465 Understanding the controlling environmental variables and soil water processes over a full crop rotation, Water Research Commission Report K5/2022, ISBN 9781431205165, South Africa, 155 pp., 2014.

Forrester, D. I., Collopy, J. J., Morris, J. D.: Transpiration along an age series of Eucalyptus globulus plantation in southeastern Australia, For. Ecol. Manage., 259, 1754-1760, https://doi.org/10.1016/j.foreco.2009.04.023, 2010.

470

Fox, T. R., Jokela, E. J., Allen, H. L.: The development of pine plantation silviculture in the southern United States, J. Forest. 105, 337–347, https://doi.org/10.1093/jof/105.7.337, 2007.

Forestry South Africa: https://www.forestry.co.za/uploads/File/industry_info/statistical_data/statistical/South%20African%2

475   0Forestry%20&%20Forest%20Products%20Industry%20-%202018.pdf, last access: 21 April 2022, 2018.

Fuchs, S., Leuschner, C., Link, R., Coners, H., Schuldt, B.: Calibration and comparison of thermal dissipation, heat ratio and heat field deformation sap flow probes for diffuse-porous trees, Agric. For. Meteo., 244-245, 151-161, https://doi.org/10.1016/j.agrformet.2017.04.003, 2017.

480

Hasenmueller, A. A., Gu, X., Weitzman, J. N., Adams, T. S., Stinchcomb, G. E., Eissenstat, D. M., Drohan, P. J., Brantley, S. L., Kaye, J. P.: Weathering of rockto regolith: The activity of deep roots in bedrock fractures, Geoderma, 300, 11-31, https://doi.org/10.1016/j.geoderma.2017.03.020, 2017.

485   Hatton, T. J, Vertessy, R. A.: Transpiration of plantation *Pinus radiata* estimated by the heat pulse method and the Bowen ratio, Hydrol. Processes, 4, 289-298, https://doi.org/10.1002/hyp.3360040309, 1990.

Hatton, T. J. and Wu, H.-I.: Scaling theory to extrapolate individual tree water use to stand water use, Hydrol. Proc., 9, 527–540, https://doi.org/10.1002/hyp.3360090505, 1995.

490

Lane, P. N., Morris, J., Zhang, N., Zhou, G., Xu, D. P.: Water balance of tropical eucalypt plantations in south-eastern China. Agric. For. Meteo., 124, 253-267, https://doi.org/10.1016/j.agrformet.2004.01.015, 2004.

Maier, C. A, Albaugh, T. J, Cook, R. I, Hall, K., McInnin, D., Johnsen, K. H., Johnson, J., Rubilar, R.A., Vose, J. M.:
495   Comparative water use in short-rotation *Eucalyptus benthamii* and *Pinus taeda* trees in the Southern United States, For. Ecol. Manage, 397, 126-138, https://doi.org/10.1016/j.foreco.2017.04.038, 2017.

Meiresonne, L., Nadezhdin, N., Cermák, J., Van Slycken, J., and ˇ Ceulemans, R.: Measured sap flow and simulated transpiration from a poplar stand in Flanders (Belgium), Agr. For. Meteorol., 96, 165–179, https://doi.org/10.1016/S0168-
500   1923(99)00066-0, 1999.

Mitchell, P. J., O'Grady, A. P., Tissue, D. T., White, D. A., Ottenschlaeger, M. L., Pinkard, E. A.: Drought response strategies define the relative contributions of hydraulic dysfunction and carbohydrate depletion during tree mortality. New Phytol., 197, 862–872, https://doi.org/10.1111/nph.12064, 2013.

505

Moran, E., Lauder, J., Musser, C., Stathos, A., Shu M.: The genetics of drought tolerance in conifers, New. Phytol., 216, 1034-1048, https://doi.org/10.1111/nph.14774, 2017.

Morris, J. D., Collopy, J. J.: Water use and salt accumulation by *Eucalyptus camaldulensis* and *Casuarina cunninghamiana*
510   on a site with shallow saline groundwater, Agric. Water Manag., 39, 205–227, https://doi.org/10.1016/S0378-3774(98)00079-1, 1999.

Mucina, L., Rutherford, M. C.: The Vegetation of South Africa, Lesotho and Swaziland, Strelitzia 19, South African National Biodiversity Institute, Pretoria, South Africa, 2006.

515

Nambiar, E. K. S.: Tamm Review: Re-imagining forestry and wood business: pathway to rural development, poverty alleviation and climate change mitigation in the tropics, For. Ecol. Manage., 448, 160–173, https://doi.org/10.1016/j.foreco.2019.06.014, 2019.

520 O'Grady, A. P., Eamus, D., Hutley, L. B.: Transpiration increases during the dry season: patterns of tree water use in eucalypt open-forests of northern Australia, Tree Physiol., 19, 591-597, https://doi:10.1093/treephys/19.9.591, 1999.

Samuelson, L. J., Farris, M. G., Stokes, T. A., Coleman, M. D.: Fertilization but not irrigation influences hydraulic traits in plantation-grown loblolly pine, For. Ecol. Manage., 255, 3331–3339, https://doi.org/10.1016/j.foreco.2008.02.014, 2008.
525

Samuelson, L. J., Stokes, T. A., Ramirez, M. R., Mendonca, C. C.: Drought tolerance of a *Pinus palustris* plantation, For. Ecol. Manage., 451, Article 117557, https://doi.org/10.1016/j.foreco.2019.117557, 2019.

Santra, P., Kumar, M., Kumawat, R. N., Painuli, D., K., Hati, K. M., Heuvelink, G. B. M., Batjes, N. H.: Pedotransfer functions
530 to estimate soil water content at field capacity and permanent wilting point in hot Arid Western India, J. Earth Syst. Sci., 127, 439–448, https://doi.org/10.1007/s12040-018-0937-0, 2018.

Savage, M. J., Everson, C. S., and Metelerkamp, B. R.: Evaporation measurement above vegetated surfaces using micrometeorological techniques, Water Research Commission Report No. 349/1/97, ISBN 1-86845 363 4, Water Research
535 Commission, Pretoria, South Africa, 248 pp., 1997.

Scott, D. F., Lesch, W.: Streamflow responses to afforestation with *Eucalyptus grandis* and *Pinus patula* and to felling in the Mokobulaan experimental catchments, South Africa, J. Hydrol., 199, 360–377, https://doi.org/10.1016/S0022-1694(96)03336-7, 1997.
540

Soares, J. V., Almeida, A. C.: Modeling the water balance and soil water fluxes in a fast-growing *Eucalyptus* plantation in Brazil. J. Hydrol., 253, 130–147, https://doi.org/10.1016/S0022-1694(01)00477-2, 2001.

Soil Classification Working Group: Soil classification: a taxonomic system for South Africa, Department of Agriculture Report
545 No. 15, Pretoria, South Africa, 257 pp., 1991.

Stanturf, J. A., Vance, E. D., Fox, T. R., Kirst, M.: *Eucalyptus* beyond its native range: Environmental issues in exotic bioenergy plantations, Int. J. For. Res. 16, https://doi.org/10.1155/2013/463030, 2013.

550 Sun, G., Noormets. A., Gavazz, M. J.: Energy and water balance of two contrasting loblolly pine plantations on the lower coastal plain of North Carolina, USA, For. Ecol. Manage., 259, 1299–1310, https://doi.org/10.1016/j.foreco.2009.09.016, 2010.

Traver, E., Ewers, B. E., Mackay, D. S., and Loranty, M. M.: Tree transpiration varies spatially in response to atmospheric but
555 not edaphic conditions, Funct. Ecol., 24, 273–282, https://www.jstor.org/stable/40603043, 2010.

Vandegehuchte, M. W. and Steppe, K.: Use of the correct heat conduction–convection equation as basis for heat-pulse sap flow methods in anisotropic wood, J. Exp. Bot., 63, 2833–2839, https://doi.org/10.1093/jxb/ers041, 2012.

560 Vertessy, R. A., Hatton, T. J., Reece, P., O'Sullivan, S. K., and Benyon, R. G.: Estimating stand water use of large mountain ash trees and validation of the sap flow measurement technique, Tree Physiol., 17, 747–756, https://doi.org/10.1093/treephys/17.12.747, 1997.

White, D. A., Beadle, C. L., Sands, P. J., Worledge, D., Honeysett, J. L.: Quantifying the effect of cumulative water stress on stomatal conductance of *Eucalyptus globulus* and *Eucalyptus nitens*: a phenomenological approach, Aust. For., 26, 17-27, http://dx.doi.org/10.1071/PP98023, 1999.

White, D. A., Silberstein, R. P., Contreras, F. B., Quiroga, J. J., Meason, D. F., Palma, J. H. N., de Arellano, P. R.: Growth, water use, and water use efficiency of *Eucalyptus* globulus and *Pinus radiata* plantations compared with natural stands of Roble-Hualo Forest in the coastal mountains of central Chile, For. Ecol. Manage., 501, 119675-119676, https://doi.org/10.1016/j.foreco.2021.119676, 2021.

White, D. A., Ren, S., Mendham, D. S., Contreras, F. B, Silberstein, R. P., Meason, D., Iroume, A., de Arellano, P. R.: Is the reputation of *Eucalyptus* plantations for using more water than *Pinus* plantations justified? Hydrol. Earth Syst. Sci., 26, 5357-5371, https://doi.org/10.5194/hess-26-5357-2022, 2022.

Whitehead, D., Beadle, C. L.: Physiological regulation of productivity and water use in Eucalyptus: a review. For. Ecol. Manage., 193, 113-140, https://doi.org/10.1016/j.foreco.2004.01.026, 2004.

WMO: Guide to Meteorological Instruments and Methods of Observation, World Meteorological Observation Report No.8, Geneva, Switzerland, 716 pp., 2010.

605

610

615

620

625

630

Figure 1. Location of the study area next to Two Streams Research Catchment. The Google Earth Pro extract (above) provides location of the two study sites, *E. grandis* x *E. nitens* (*GN*), *Pinus elliottii* and the automatic weather station (© Google Maps 2022).

635

640

655
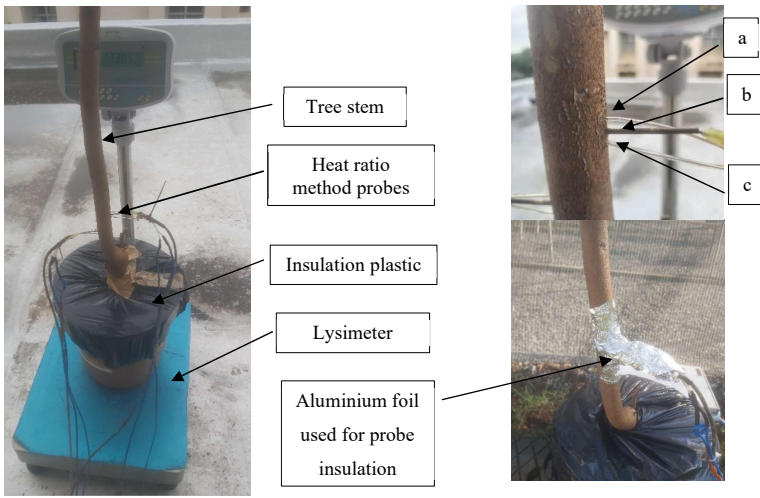
Figure 2. An illustration of a calibration experiment setup showing a tree installed with the heat ratio probes, placed in a lysimeter. Insert: a= downstream probe, b= heater probe, c= upstream probe with aluminium foil used for insulation.

660

665

670

675
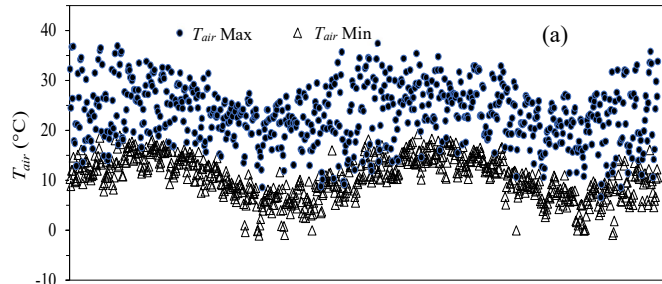
680
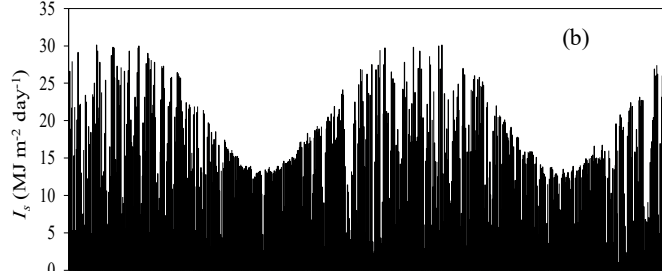
685
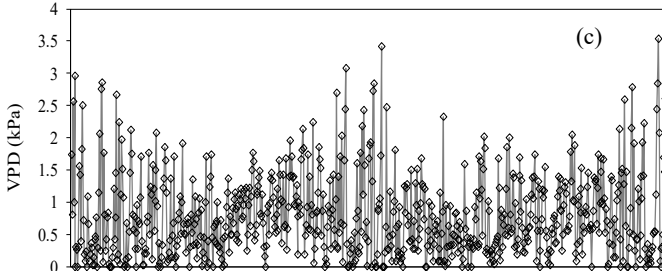
690
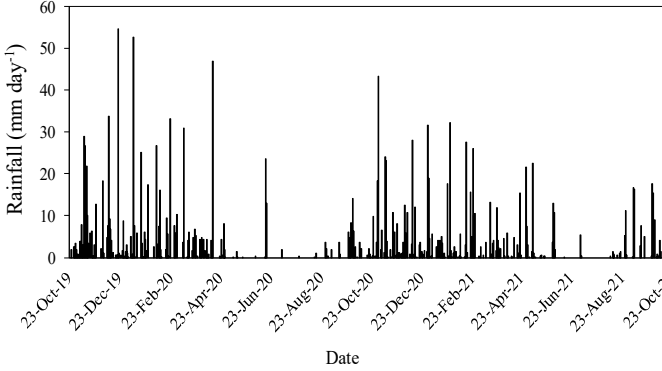
695

700

705
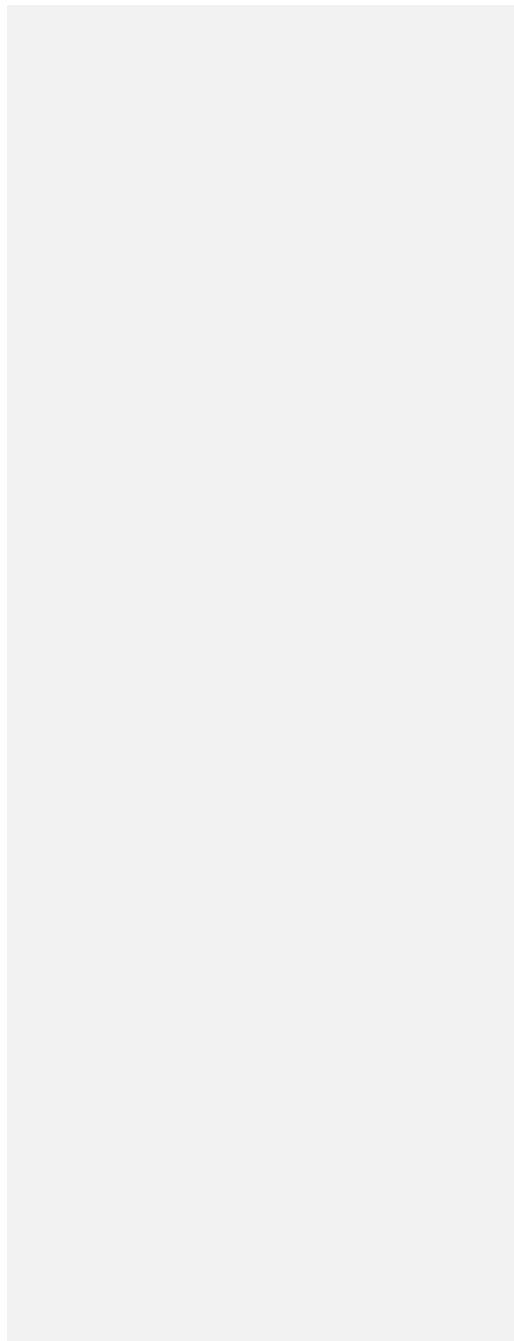
Figure 3. (a) the daily minimum (T_{air} Min) and maximum (T_{air} Max) air temperature (°C) (b) daily total solar irradiance (I_s, MJ m^{-2} day^{-1}) (c) daily mean vapour pressure deficit (VPD, kPa) and (d) total daily rainfall (mm day^{-1}) for a duration October 2019 to October 2021.
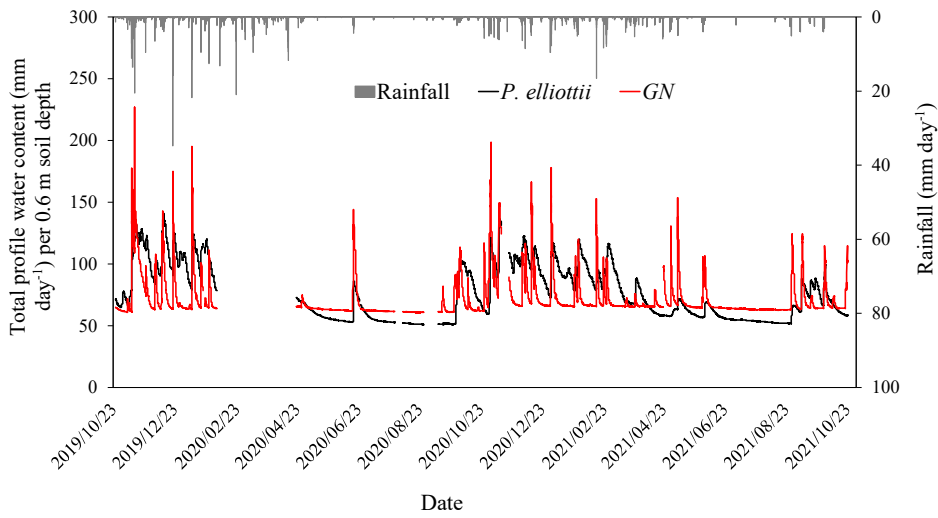
Figure 4. The total profile water content (mm day^{-1}) measured in the top 0.6 m of the soil profile in the *Pinus elliottii* and *Eucalyptus grandis* x *E. nitens* clonal hybrid sites in response to rainfall events (mm day^{-1}) during the period October 2019 to October 2021. A gap in the graph indicates a missing data.

725

730

735

740

745

750
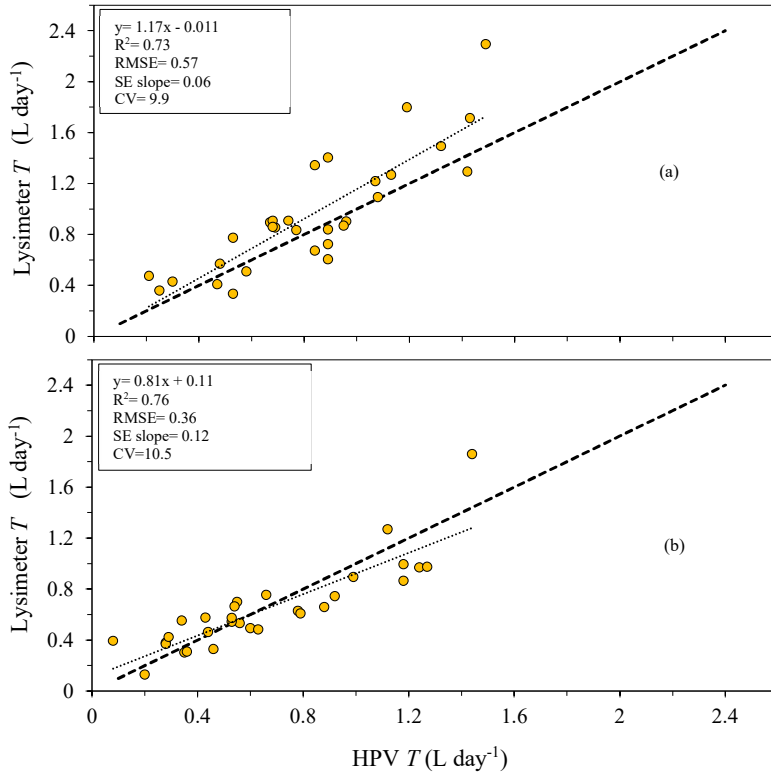
Figure 5. Relationship between daily transpiration (T) measured using a heat ratio technique (HPV, L day^{-1}) and the T measured using a lysimeter (through a change in mass, L day^{-1}) for (a) two-year-old *Eucalyptus grandis* x *Eucalyptus nitens* clonal hybrid and (b) three-year-old *Pinus elliottii*. The equation of the regression line, regression coefficient (R^2), root mean square error (RMSE), standard error of the regression slope (SE slope) and coefficient of variation (CV) for each specie is presented. The dashed line is the 1:1 line.

755
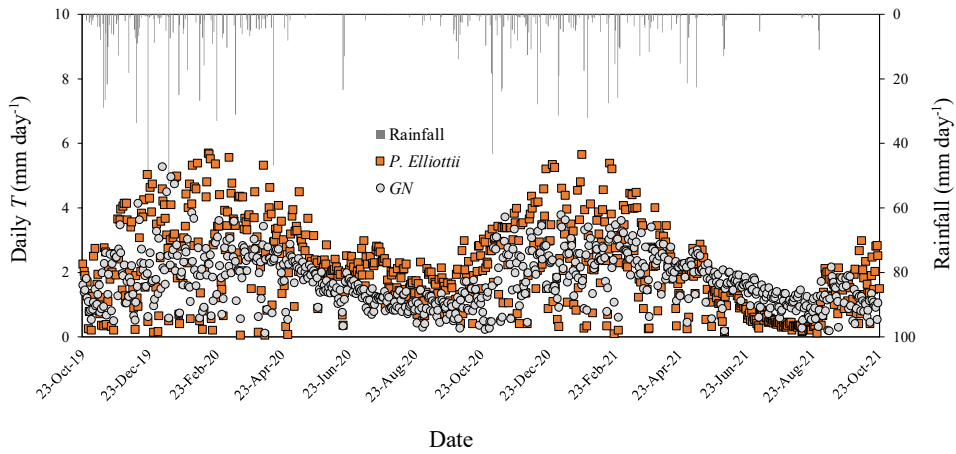
760 **Figure 6.** Mean daily transpiration $(T$, mm day$^{-1})$ and corresponding rainfall $(mm day^{-1})$ in an 8-year-old *E. grandis* x *E. nitens* clonal hybrid (*GN*) and 20-year-old *P. elliottii* trees for a duration October 2019 to October 2021. Each point is a mean of four trees.
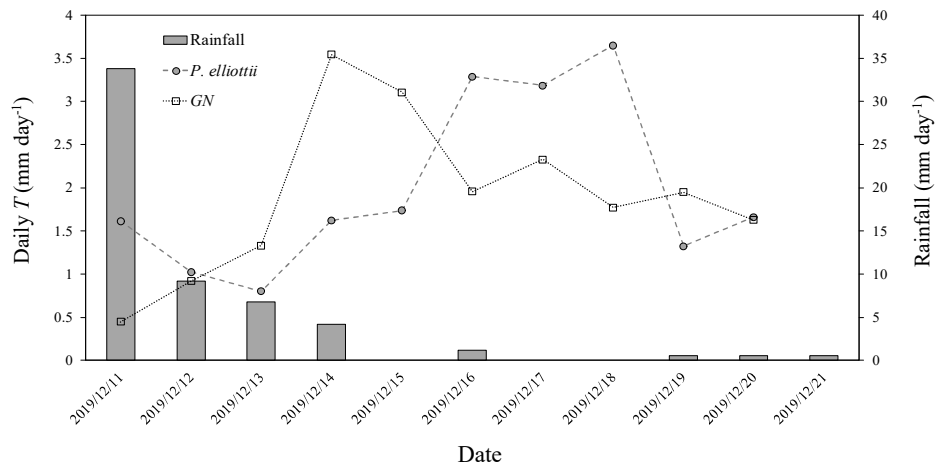
Figure 7. Ten-day daily transpiration (T, mm day^{-1}) for 20-year-old *P. elliottii* and 8-year-old *Eucalyptus grandis* x *Eucalyptus nitens* clonal hybrid (*GN*) with corresponding rainfall (mm day^{-1}) showing T response by each specie to rainfall.
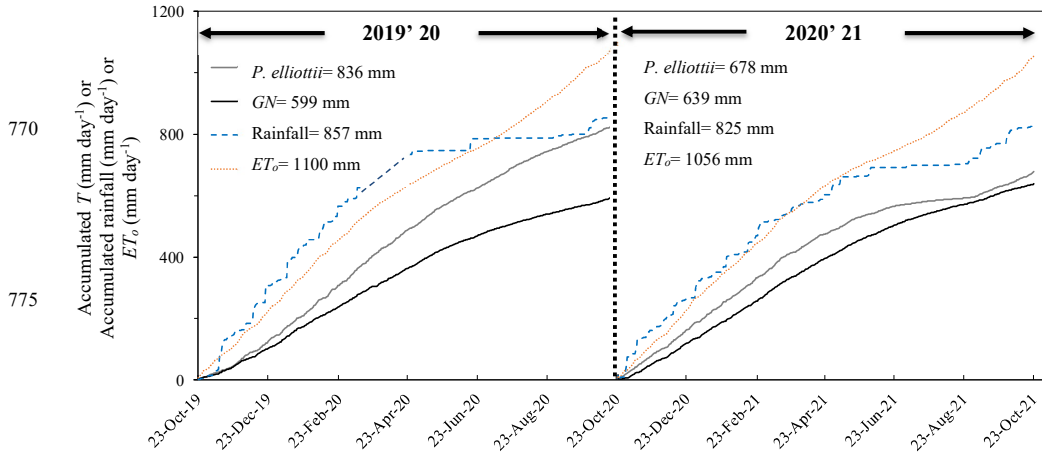
Figure 8. The accumulated transpiration (T, mm day^{-1}), rainfall (mm day^{-1}) and FAO reference evaporation (ET_o, mm day^{-1}) for 2019' 20 hydrological year (Oct 2019 to Oct 2020) and 2020' 21 hydrological year (Oct 2020 to Oct 2021).

Date
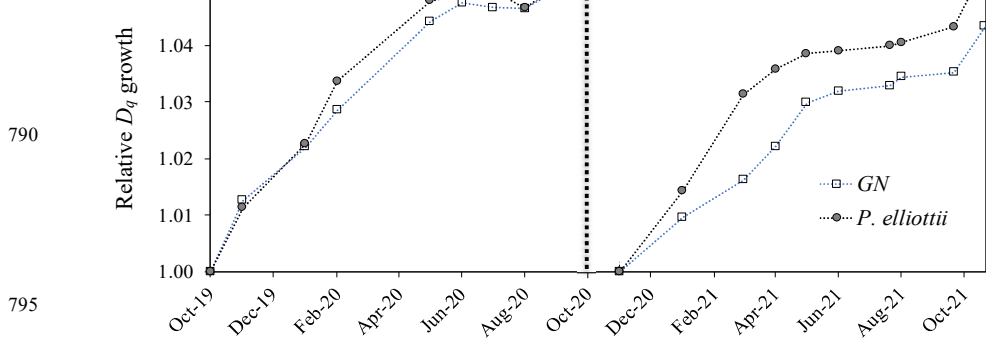
800   **Figure 9.** Relative quadratic mean diameters (D_q, normalised) measured using manual dendrometers bands for *Eucalyptus grandis* x *E. nitens* (*GN*) and *Pinus elliottii*. Measurements were conducted in two hydrological years, 2019' 20 (October 2019 to October 2020) and 2020' 21 (October 2020 to October 2021). Each point represents an average of 48 trees for each specie.
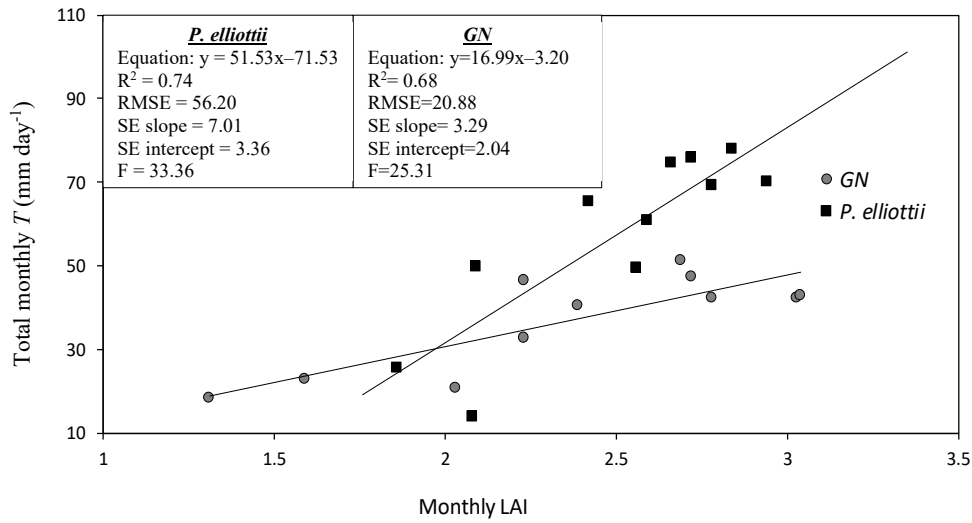
805   **Figure 10.** A linear relationship between total monthly transpiration (T, mm day^{-1}) and monthly measured leaf area index (LAI) for *Eucalyptus grandis* x *E. nitens* clonal hybrid (*GN*) and *Pinus elliottii*. The equation of the regression line, regression coefficient (R^2), root mean square error (RMSE), the standard error of the regression slope (SE slope), the standard error of the y- intercept (SE intercept) and the ratio of variance (F) for each specie is presented.

810

815

Table 1. The general characteristics of the two study sites at Mistley Canema. The abbreviations MAP and MAT denotes mean annual precipitation and mean annual temperature, respectively.

	Study sites	
Characteristics	*P. elliottii*	*GN*
Lithology	Arenite	Arenite
Soil texture	Sandy loam	Sandy clay
Bulk density (g.cm^3)	1.33	1.17
Altitude	884	976
Climate	Warm temperate	Warm temperate
MAP (mm)	800 – 1200	800 – 1200
MAT (°C)	17	17

820

Table 2. A description of soil characteristics adjacent to our study site (sourced from Clulow et al. 2014).

Horizons	Approximate depth (m)
Orthic A	0 – 2.5 m
Red apedal B	2.6 – 13 m
Saprolite	14 – 20 m
Grey fine-grained shale	21 – 40 m
Grey fractured basement granite	41 – 80 m

825 **Table 3.** Detailed description of trees monitored on *Pinus elliottii* and *Eucalyptus grandis* x *E. nitens* clonal hybrid (*GN*) study sites.

Trees	Overbark diameter (cm)		Bark (cm)		Sap-wood depth (cm)		Probe depth under bark surface (cm)	
	P. elliotti	*GN*	*P. elliotti*	*GN*	*P. elliotti*	*GN*	*P. elliotti*	*GN*
Tree 1	10.7	10.5	2.2	0.7	4.88	2.55	1	1
Tree 2	15.9	11.4	2.4	0.8	7.2	2.8	2	1.5
Tree 3	18.2	12.5	2.4	0.8	8.3	3.0	3	2.5
Tree 4	22.4	14.2	2.5	0.9	10.2	3.9	4	3.5

830   **Table 4.** Statistical significance (*p*-values derived ANOVA tests) of the *Eucalyptus grandis* x *E. nitens* (*GN*) *and Pinus elliottii* hourly mean transpiration over 2019' 20 and 2020' 21 hydrological years (summer = November to February and winter = June to July) versus the mean hourly climatic variables (I_s= solar radiation, VPD=vapour pressure deficit, *RH*=relative humidity, WS=wind speed and T_{air}=air temperature). Statistically significant ($p < 0.05$) values are shown in bold type.

	Species	Season	I_s	VPD	Rain	*RH*	WS	T_{air}
					Dependant variable			
2019' 20	*GN*	Summer	**<0.001**	**0.005**	0.56	0.13	0.27	0.39
		Winter	0.58	0.07	0.23	0.09	0.23	0.28
	P. elliottii	Summer	**<0.001**	0.67	0.30	0.35	0.21	0.12
		Winter	**0.03**	0.81	0.71	**0.03**	0.27	0.58
2020' 21	*GN*	Summer	**<0.001**	**<0.001**	0.29	0.30	0.71	0.12
		Winter	**0.006**	0.93	0.12	0.33	0.06	0.53
	P. elliottii	Summer	**0.002**	0.43	0.37	**0.04**	0.48	0.30
		Winter	0.11	0.50	0.65	0.77	0.26	0.24

835

840